ELSEVIER

Chemical Engineering Science 62 (2007) 878–898

Chemical Engineering Science

www.elsevier.com/locate/ces

Design and control of reactive distillation for ethyl and isopropyl acetates production with azeotropic feeds

I-Kuan Lai[a], Shih-Bo Hung[b], Wan-Jen Hung[a], Cheng-Ching Yu[a], Ming-Jer Lee[b], Hsiao-Ping Huang[a,*]

[a]*Department of Chemical Engineering, National Taiwan University, Taipei 106-17, Taiwan*
[b]*Department of Chemical Engineering, National Taiwan University of Science and Technology, Taipei 106-07, Taiwan*

Received 30 March 2006; received in revised form 17 August 2006; accepted 17 October 2006
Available online 29 October 2006

Abstract

Reactive distillations for the production of ethyl acetate (EtAc) and isopropyl acetate (IPAc) are classified as the type-II process where the first column consists of a reactive zone and a rectifying section followed by a stripper [Tang et al., 2005. Design of reactive distillations for acetic acid esterification with different alcohols. A.I.Ch.E. Journal 51, 1683–1699]. Instead of using pure alcohols and acetic acid as reactants, this paper studies the effects of reactant purity on the design and control of reactive distillation. This offers significant economical incentives (by reducing raw materials costs), because ethanol forms an azeotrope with water at 90 mol% and isopropanol/water has an azeotrope at 68%. The purities of the acid is set to 95% for acetic acid (industrial grade), 87% for ethanol, and 65% for isopropanol. The results show that the total annual costs (TAC) increase by a factor of 5% for EtAc and 8% for IPAc production using reactive distillation. Next, the operability of the reactive distillations with azeotrope feeds is explored. Three disturbances, feed flow, acid feed purity, and alcohol feed composition, are introduced to assess control performance using dual-temperature control and one-temperature-one-composition control. Simulation results indicate good control performance can be achieved for reactive distillation with azeotropic feeds.
© 2006 Elsevier Ltd. All rights reserved.

Keywords: Ethyl acetate; Isopropyl acetate; Azeotrope; Reactive distillation; Control; Design

1. Introduction

Esters are of great importance to chemical process industries. Among them, acetate esters are important organic solvents widely used in the production of varnishes, ink, synthetic resins, and adhesive agents. They are produced from the reactions of acid and alcohols under an acidic condition. A key issue in the production of these esters is the low conversion from the reactions. As a result, heavy capital investments and high energy costs are inevitable. The reactive distillation is a very attract way to reduce these investments and energy costs.

Keyes (1932), among the first, studied an ethyl acetate (EtAc) process using a reactive distillation column which consists of a pre-esterification reactor, two recovery columns, and a decanter. Succeeding researches on this reactive distillation have been reported on either steady-state simulations (e.g. Chang and Seader, 1988; Simandl and Svrcek, 1991; Bock et al., 1997; Giessler et al., 2001), dynamic modelling (e.g. Alejski and Duprat, 1996), operation and control (e.g. Vora and Daoutidis, 2001; Georgiadis et al., 2002), and single column experiment (e.g. Klöker et al., 2004; Kenig et al., 2001). There is a common difficulty encountered in those studies due to the existence of a three-component azeotrope that has minimum boiling point. A conventional reactive distillation column will not be able to produce high purity of the acetate due to this fact. The resulting designs, as a consequence, still lead to heavy capital investments and high operational costs. Tang et al. (2003) change the typical reactive column configuration and developed a new process that consists of two columns (i.e., a column with a reactive zone and a rectifying section (the RD column) and one stripper) to produce high purity of EtAc with

* Corresponding author. Tel.: +886 2 2363 8999; fax: +886 2 2362 3040.
E-mail address: huanghpc@ntu.edu.tw (H.-P. Huang).

0009-2509/$ - see front matter © 2006 Elsevier Ltd. All rights reserved.
doi:10.1016/j.ces.2006.10.019

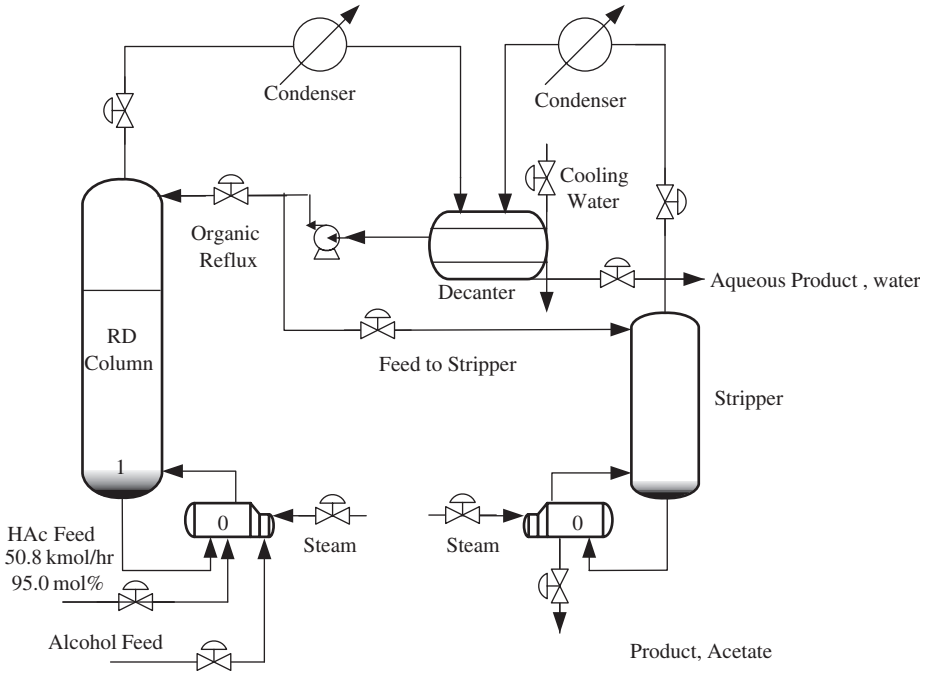

Fig. 1. Configuration of Type II process for the production of Ethyl and isopropyl acetates.

a very stringent specification on the remaining HAc. Later, it was found (Tang et al., 2005) that the production of isopropyl acetates (IPAc) encountered the same difficulty when reactive distillation is involved. Thus, Tang et al. (2005) provides a generalization from their studies of esterifications from acetic acid with different alcohols. They classified the reactive distillation column for the productions of EtAc and IPAc as a type II configuration (Fig. 1). The process configuration of this type is very different from what is known as a typical reactive distillation column. That is, instead of having reactive, rectifying, and stripping sections in one column, reaction and rectifying take place in the RD column and the further purification of acetate is carried out in a downstream stripper while recycling organics with a composition close to ternary azeotrope back to the decanter.

The objective of this work is to investigate the effects of feed purity to the design and control of type II reactive distillation for EtAc and IPAc productions. This has important economical implications, because ethanol forms an azeotrope with water at 90 mol% and isopropanol–water has an azeotrope at 68 mol% isopropanol. In addition to impure alcohol composition, the industrial grad HAc is used. Thus, without further purification on these raw materials, significant cost reduction can be achieved. The catalysts in use are Purolite CT179 in the production of EtAc system, and Amberlyst 15 in the production of IPAc. For the feed purity changes, it is important to study the possible changes in design, variations in the total annual cost (TAC), and control, disturbance rejection capability for feed flow and feed composition changes.

The remainder of this paper is organized as the follows. First, the physical properties and reaction kinetics of these two systems are investigated. Next, qualitatively, process flowsheets are generated based on the thermodynamic behaviors of these two systems. Then, design procedures are proceeded to determine, quantitatively, the numbers of trays in each of sections in the reactive distillation column and the stripper. An improved design is sought by minimizing the TAC. Finally, two control schemes (dual-temperature control and one-temperature-one-composition control) are devised and disturbance rejection capability is evaluated for flow as well as composition variations.

2. Phase equilibrium and reaction kinetics

Both the EtAc and IPAc systems exhibit non-ideal phase behaviors and, as will be shown later, each system has four azeotropes. In order to represent accurately the phase equilibriums of the systems, the selection of the form of the thermodynamic model and the determination of the parameters are essential. To account for the non-ideal vapor–liquid equilibrium (VLE) and possible vapor–liquid–liquid equilibrium (VLLE) for these quaternary systems, the NRTL (non-random two-liquid) activity coefficient model is adopted by Aspen Plus (2001).

The NRTL model parameter sets as shown in Table 1 are taken from the literature. The vapor phase non-ideality such as the dimerization of acetic acid is also considered. The second viral coefficients of Hayden-O'Connell (1975) are used to account for vapor phase association of acetic acid due to dimerization and trimerization. The Aspen Plus built-in association parameters are used to compute the fugacity coefficients.

The thermodynamic model predicts three binary and minimum boiling azeotropes and one ternary minimum boiling

Table 1
The NRTL model coefficients for EtAc and IPAc systems

Comp. i	HAc(1)	HAc(1)	HAc(1)	EtOH(2)	EtOH(2)	EtAc(3)
Comp. j	EtOH(2)	EtAc(3)	H_2O(4)	EtAc(3)	H_2O(4)	H_2O(4)
(*A*) *EtAc system*						
a_{ij}	0	0	−1.9763	1.817306	0.806535	−2.34561
a_{ji}	0	0	3.3293	−4.41293	0.514285	3.853826
b_{ij} (K)	−252.482	−235.279	609.8886	−421.289	−266.533	1290.464
b_{ji} (K)	225.4756	515.8212	−723.888	1614.287	444.8857	−4.42868
c_{ij}	0.3000	0.3000	0.3000	0.1000	0.4000	0.3643
(*B*) *IPAc system*						
Comp. i	HAc(1)	HAc(1)	HAc(1)	IPOH(2)	IPOH(2)	IPAc(3)
Comp. j	IPOH(2)	IPAc(3)	H_2O(4)	IPAc(3)	H_2O(4)	H_2O(4)
b_{ij} (K)	−141.644	70.965	−110.580	191.086	20.057	415.478
b_{ji} (K)	40.962	77.9	424.060	157.103	833.042	1373.46
c_{ij}	0.3048	0.301	0.299	0.3	0.325	0.3

Table 2
The compositions and temperatures of the azeotropes for EtAc and IPAc systems

Comp. i	Exp.[b] components	Exp.[b] temp. (°C)	Computed components	Computed temp. (°C)
EtOH/EtAc	(0.462, 0.538)	71.81	(0.4572, 0.5428)	71.81
EtOH/H_2O	(0.9037, 0.0963)	78.174	(0.9016, 0.0984)	78.18
EtAc/H_2O[a]	(**0.6885, 0.3115**)	**70.38**	(**0.6869, 0.3131**)	**70.37**
EtOH/EtAc/H_2O	(0.1126, 0.5789, 0.3085)	70.23	(0.1069, 0.6073, 0.2858)	70.09
IPOH/IPAc	(0.6508, 0.3492)	80.1	(0.5984, 0.4016)	78.54
IPOH/H_2O	(0.6875, 0.3125)	82.5	(0.6691, 0.3309)	80.06
IPAc/H_2O[a]	(**0.5982, 0.4018**)	**76.6**	(**0.5981, 0.4019**)	**76.57**
IPOH/IPAc/H_2O	(0.1377, 0.4938, 0.3885)	75.5	(0.2377, 0.4092, 0.3531)	74.22

[a]Heteroazeotropes in boldface.
[b]Experimental data (Horsley, 1973).

azeotrope for both systems. The temperatures and the compositions of these azeotropes are given in Table 2. The results clearly indicate good agreements between model prediction and experimental data. Notice that both the EtAc and the IPAc systems have a ternary minimum boiling azeotrope (i.e., EtOH–EtAc–H_2O and IPOH–IPAc–H_2O). These ternary azetropes were shown in the RCM diagrams of Tang et al. (2005). In the RCM diagrams, it was found that there are significant two-liquid (LL) envelopes. For EtAc system, the ternary minimum boiling azeotrope lies closely to the boundary of LL envelope, while for the IPAc system, the ternary minimum boiling azeotrope lies well inside the envelope. It is interesting to see that, in both systems, the tie lines slope toward pure water node and, consequently, relatively pure water can be recovered from the LL separation in these two esterification processes. This implies that a decanter can be installed to recover one of the products, water. This will be addressed further in the next section.

The alcohols studied in this work include ethanol (EtOH) and isopropyl alcohol (IPOH), and the products are EtAc and IPAc, respectively. The reactions are reversible:

For EtAc system:

$$EtOH + HAc \underset{k_{-1}}{\overset{k_1}{\rightleftarrows}} EtAc + H_2O.$$

For IPAc system:

$$IPOH + HAc \underset{k_{-1}}{\overset{k_1}{\rightleftarrows}} IPAc + H_2O.$$

The solid catalysts in use are the acidic ion-exchange resin Purolite CT179 and Amberlyst 15 (Rohm and Hass), respectively. The reaction rates are expresses in the pseudo-homogeneous model or Langmuir–Hinshelwood model (see Table 3, Hangx et al., 2001; Gadewar et al., 2002). Notice that, in the Langmuir–Hinshelwood model, the component is represented in terms of activity and both are all catalyst-weight-based (m_{cat}). The catalyst weight is computed by assuming that the solid catalyst occupies 50% of the tray holdup and a catalyst density of 770 kg/m^3 is used to convert the volume into catalyst-weight (m_{cat}). Before leaving this section, it should be noted here that Aspen Plus does not support activity-based

Table 3
Kinetic equations for EtAc and IPAc systems

System	Kinetic model (catalyst)	k_1 ($T = 363$ K)	K_{eq} ($T = 363$ K)
(A) EtAc	Pseudo-homogeneous model (Purolite CT179) $r = m_{cat}(k_1 x_{HAc}^{1.5} x_{EtOH} - k_{-1} x_{EtAc} x_{H_2O})$ $k_1 = 4.24 \times 10^3 \exp\left(\frac{-48300}{RT}\right)$ $k_{-1} = 4.55 \times 10^5 \exp\left(\frac{-66200}{RT}\right)$	4.78×10^{-4} [k mol/(kg$_{cat}$[a] s)]	3.50
(B) IPAc	Langmuir–Hinshelwood/Hougen–Watson model (Amberlyst 15) $r = m_{cat} \frac{k_1(a_{HAc}a_{IPOH} - a_{IPAc}a_{H_2O}/K_{eq})}{(1 + K_{HAc}a_{HAc} + K_{IPOH}a_{IPOH} + K_{IPAc}a_{IPAc} + K_{H_2O}a_{H_2O})^2}$ $k_1 = 7.667 \times 10^{-5} \exp\left(23.81 - \frac{68620.43}{RT}\right)$ $K_{eq} = 8.7, \quad K_{HAc} = 0.1976, \quad K_{IPOH} = 0.2396, \quad K_{IPAc} = 0.147,$ $K_{H_2O} = 0.5079$ Assumption: mol H + /kg$_{cat}$ $= 4.6 \times 10^{-3}$	2.26×10^{-4} [k mol/(kg$_{cat}$[a] s)]	8.7

[a] $R = 8.314$ [kJ/k mol/K], T[K], r[k mol/s], m_{cat} [kg$_{cat}$], x_i[mole fraction].
(A) Hangx et al. (2001), (B) Gadewar et al. (2002).

reaction kinetics and, therefore, a FORTRAN subroutine should be written to compute the extent of reaction in each tray.

3. Process flowsheet and steady-state design

3.1. Flowsheet

A common phase-equilibrium characteristic shared by the EtAc and IPAc systems is that they have a LL envelope with tie lines mostly point to the high-purity H_2O corner. This phenomenon is even more obvious in the system of the IPAc system. It was found that, in this type of process, the reactive zone extends to the column base in the first column (called the RD column) and, therefore, a much larger holdup is expected in the bottom of the RD column. This is advantageous from reaction perspective, because we have a large reactor with high reaction temperature (as a result of column base). In this work, the column base holdup is taken to be 10 times of the tray holdup. The reactive section generates necessary acetates followed by a rectifying section in which the composition of the heavy acid (HAc) is kept to a ppm level. The specifications include: 50 kmol/h of ester products with purity level of 99 mol% while keeping acid purity below 100 ppm. In this study, the feed composition of alcohols are set to 87 mol% for EtOH and 64.91 mol% for IPOH, respectively. The alcohol purity level is slightly less than corresponding alcohol azeotropic composition. Industrial grade acetic acid is used and this corresponds to 95 mol% with water as impurity in both systems. Notice that the overhead composition of the RD column approaches the ternary azeotrope composition as a result of the minimum boiling point. Because the acid composition decreases toward the top of the RD column, the column profile will approach the azeotrope from the alcohol lean direction (refer to the RCM's by Tang et al., 2005) as will be confirmed later in the distillation lines. This is helpful to remove water via liquid–liquid separation. The composition of organic phase is similar to that of overhead. Thus, a decanter is placed for water removal and part of the organic phase is recycled back to the RD column while feeding the organic distillate to a stripper for further purification. The top of the stripper is also recycled back to the decanter. The conceptual design of the EtAc and IPAc is shown in Table 4. Steady-state simulation shows that this flowsheet is feasible and a straightforward separation between the acetates and the alcohols is conducted in the stripper that leads to high purity of EtAc and IPAc as products in the bottom of the stripper (the upper corner distillation region in the RCM's). The purity level of the acid in the product stream depends on the amount of acid allowed in the overhead of the RD column.

3.2. Design procedure

Based on this process flowsheet, a procedure is used to achieve an improved design to reduce the TAC. Similar design procedure was also taken by Tang et al. (2005) for design. Because of the stringent requirement of the acid level in the product, the stoichiometric ratio of the reactants is allowed to vary. This leads to the following design variables: number of trays in the reactive zone (N_{rxn}), number of trays in the rectifying section (N_r), feed tray locations of the light and heavy reactants (NF_{heavy} and NF_{light}), feed ratio of two reactants (FR), and number of trays in the stripper (N_s). Two manipulating variables considered here include reflux ratio of RD column and reboiler duty of stripper. In the search of improved designs for these two processes, all the simulations are carried out using

Table 4
Results of steady-state designs of EtAc and IPAc systems

System	(A) EtAc		(B) IPAc	
Column configuration	RD column	Stripper	RD column	Stripper
Total no. of trays including the reboiler	20	10	24	8
No. of trays in stripping section (N_s)		9		7
No. of trays in reactive section (N_{rxn})	11		14	
No. of trays in rectifying section (N_r)	9		10	
Reactive tray	0–10		0–13	
Acetic acid feed tray	0		0	
Alcohol feed tray	0		0	
Feed flow rate of acid (kmol/h)	50.80		50.74	
Feed flow rate of alcohol (kmol/h)	57.47		77.03	
Top product flow rate (kmol/h)	60.45		79.73	
Bottom product flow rate (kmol/h)		47.82		46.97
X_D or $X_{D,\mathrm{aq}}$				
Acid (m.f.)	0.00001		1.08E−6	
Alcohol (m.f.)	0.02182		0.02946	
Acetate (m.f.)	0.01498		0.0085	
Water (m.f.)	0.96391		0.9619	
X_B				
Acid (m.f.)		0.00010		0.0001
Alcohol (m.f.)		0.00912		0.00986
Acetate (m.f.)		0.99000		0.99000
Water (m.f.)		0.00078		0.00004
X_{ORG}				
Acid (m.f.)	0.00002		0.00002	
Alcohol (m.f.)	0.05680		0.017240	
Acetate (m.f.)	0.71480		0.59950	
Water (m.f.)	0.22840		0.22790	
Reflux ratio	1.76		1.48	
Condenser duty (kW)	−4789.92	−1668.73	−3951.00	−1301.63
Subcooling duty (kW)	−881.45		−564.87	
Reboiler duty (kW)	5113.4	1979.01	4014.17	1557.66
Column diameter (m)	2.043	1.37	1.94	1.3
Weir height (m)	0.1016	0.0508	0.1016	0.0508
Decanter temperature(°C)	40		50	
Condenser heat transfer area (m^2)	177.1	61.85	126.73	42.26
Subcooling heat transfer area (m^2)	179.96		76.52	
Reboiler heat transfer area (m^2)	190.7	83.65	149.69	65.83
Damköhler number (Da)	30.94		14.03	
Total capital cost ($1000)	2103.01		1779	
Column	521.4		531.3	
Column trays	91.42		95.08	
Heat exchangers	1490.2		1151.9	
Total operating cost ($1000/year)	656.10		533.8	
Catalyst cost	71.30		74.2	
Energy cost	584.90		459.6	
TAC ($1000/year) (50 kmol/h)	1357.12		1126.8	
TAC ($1000/year) (52 825 ton/year)	1993.64		1377.95	

Aspen Plus with the RADFRAC module provided with a FORTRAN subroutine for the reaction rates. By giving a production rate and product specifications, the steps in the following are adopted to obtain a near optimal design:

(1) Set the reactants feed ratio to 1 initially (i.e., $FR = F_{\mathrm{Acid}}/F_{\mathrm{Alcohol}} = 1$).
(2) Fix a number of reactive trays (N_{rxn}).
(3) Place the heavy reactant feed (NF_{Acid}) on the top of the reactive zone and introduce the light reactant feed (NF_{Alcohol}) on the lowest tray of the reactive zone.
(4) Guess the tray numbers in the rectifying section (N_r) and the stripping section (N_s).
(5) Change the organic reflux flow (R) and stripper heat input ($Q_{R,S}$) (type II flowsheet) until the product specification is met.

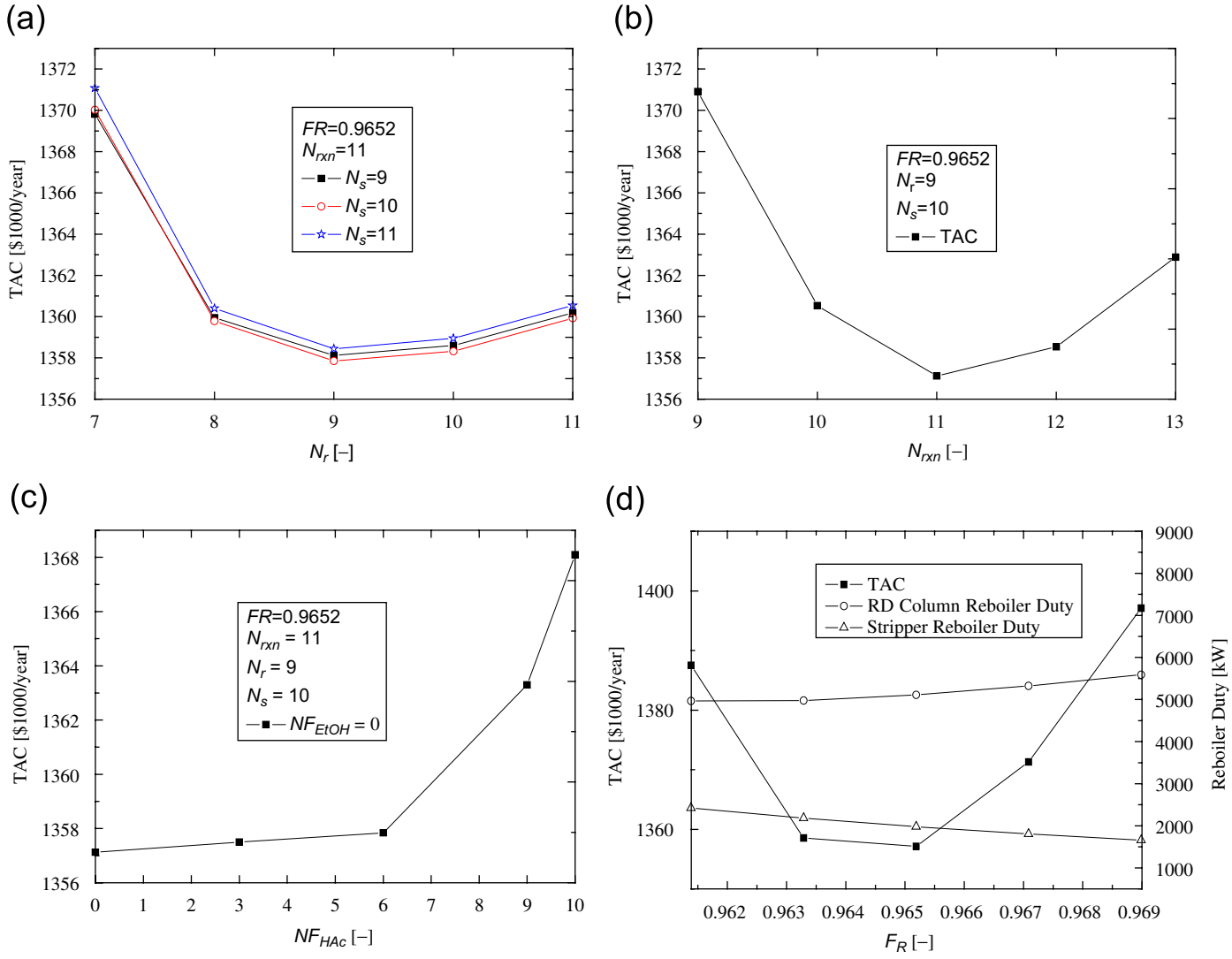

Fig. 2. Effects of design variables, (a) number of trays in rectify section (N_r), (b) number of reactive trays (N_{rxn}), (c) acetic acid feed tray location (NF_{HAc}) and (d) feed ratio (FR) on TAC for the EtAc system.

(6) Go back to (4) and change N_r and N_s until the TAC is minimized.
(7) Go back to (3) and find the feed locations (NF_{Acid} and $NF_{Alcohol}$) until the TAC is minimized.
(8) Go back to (2) and vary N_{rxn} until the TAC is minimized.
(9) Go back to (1) and change the feed ratio (FR) until the TAC is minimized.

The TAC used to evaluate for the resultant design is expressed as

$$\text{TAC} = \text{operating cost} + \frac{\text{capital cost}}{\text{payback year}}.$$

Here the operating cost includes the costs of steam, cooling water, and catalyst, and the capital cost covers the cost of the column, trays, and exchangers and reboilers. A payback year of 3 is used here.

The above-mentioned design procedure follows the direct search method proposed by Hooke and Jeeves (1966) in search of a minimum TAC. Similar procedure was adopted in the design of other RD processes (e.g. Tang et al., 2005). This direct search method was not considered as efficient as some late methods such as MINLP and MIDO for optimizing an objective function subjected to constraints of algebraic equations or differential-algebraic equations (abbr. DAE). Nevertheless, it is simple, direct and bounded for a near optimal result, especially in search with models simulated by some commercial simulation packages (e.g. Aspen Plus).

3.3. Results

The results of steady-state design of these two processes are given in Table 4. The process flowsheets thus obtained are given in Table 4 with corresponding flow rates and composition. The

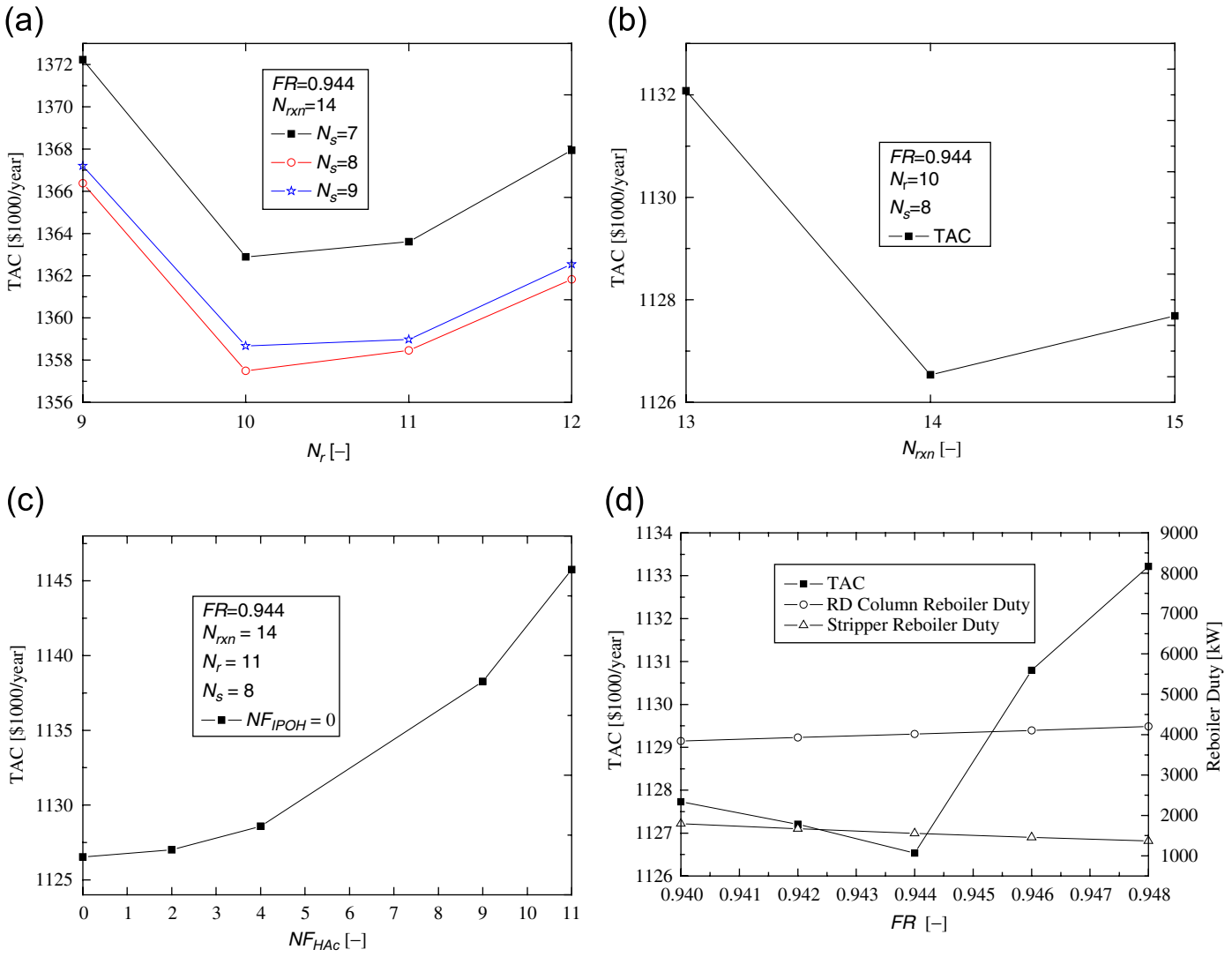

Fig. 3. Effects of design variables, (a) number of trays in rectify section (N_r), (b) number of reactive trays (N_{rxn}), (c) acetic acid feed tray location (NF_{HAc}) and (d) feed ratio (FR) on TAC for the IPAc system.

designs correspond to organic reflux ratio of 1.76 for the EtAc and 1.48 for the IPAc, respectively.

From Figs. 2 and 3, it is found that the number of trays in the rectifying section of RD column (i.e., N_r) is an important design variable. On the other hand, the number of trays in the stripper (i.e., N_s) has little impact on the TAC when N_r is fixed. It is also observed that the locations of the feed tray for both the acid and the alcohol are also very important variables. It turns out that both feeds enter at the reboiler is most advantageous as far as the TAC is concerned. The reason for that is: the largest catalyst holdup is placed in the reboiler of the RD column where higher concentrations of both reactants will be beneficial for the reaction. Fig. 4 shows concentration profiles throughout the RD column. The area with gray shadow show also the fraction of reaction takes place in each tray. Even though almost about 80% of reactions take place in this reboiler, the remaining 20% of reaction takes place in the RD column cannot be neglected. Without this remaining 20% of reaction in the RD column, the conversion of HAc will not be high enough to meet its specification in the top. Another dominant variable found for design is the feed ratio (FR) of the two reactants. The result shows that a little alcohol excess is favorable because this helps to consume up all the acid and to meet the stringent acid spec for acetates. In doing this, the overhead condensate falls into LL zone and, thus, most of the water can be separated in the decanter that leads to a significant energy saving. It is interesting to note that both systems exhibit similar characteristic in the design as shown in Fig. 4.

The composition profiles of both processes are given in Fig. 4. As pointed out earlier, most of the reactions take place in the reboiler in both cases. In each system, nevertheless, there is still a small portion of reaction taking place in the RD column. This portion of reaction is important, because, by this reaction, it consumes up the remaining acid in the RD column so that only a nearly ternary water–alcohol–acetate system appears at the column top. The condensate has liquid–liquid phase and is

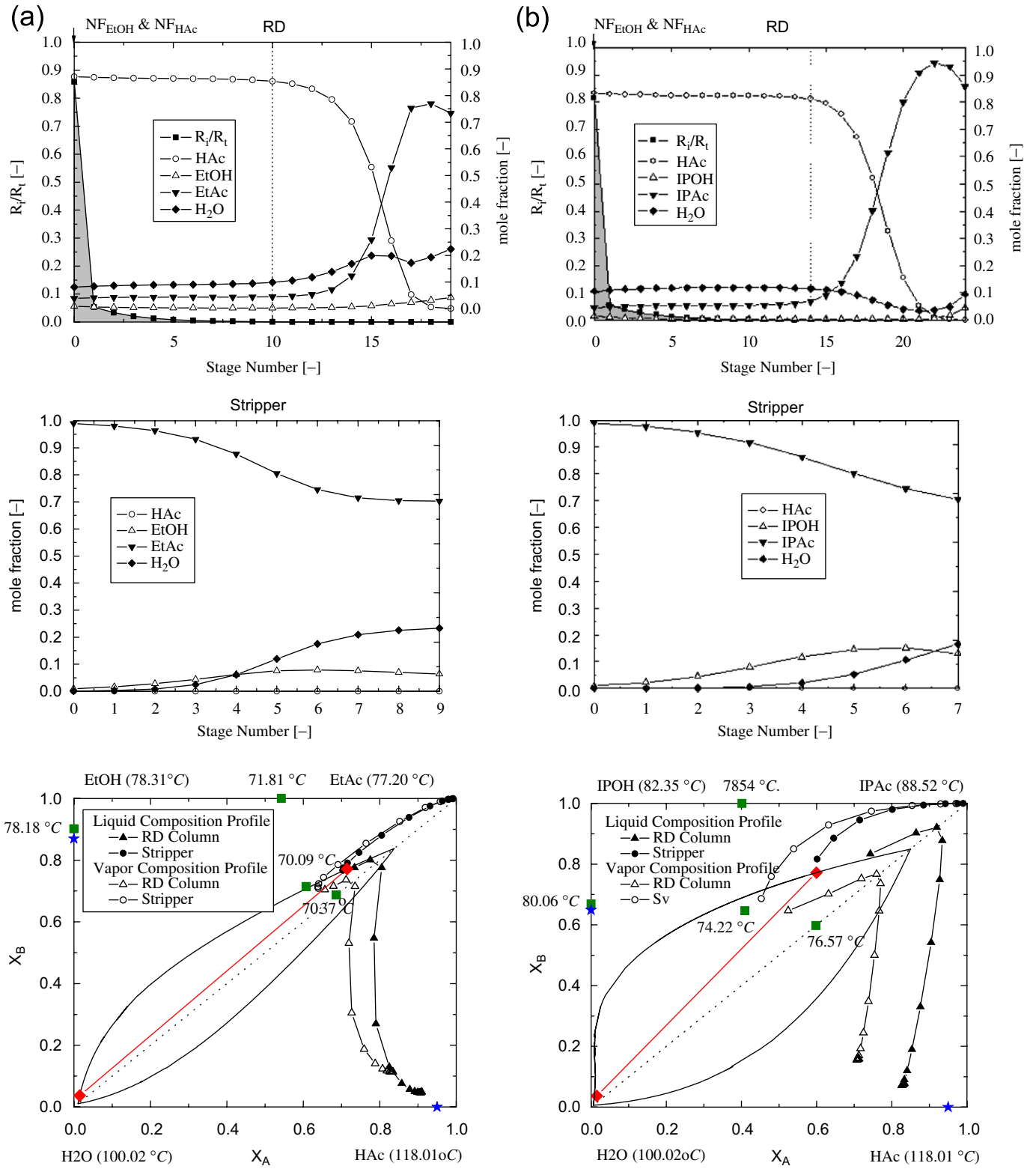

Fig. 4. Composition profiles of both systems: RD column, stripper and transformed liquid and vapor composition in the quaternary system ($X_A = X_{\text{HAc}} + X_{\text{Acetate}}, X_B = X_{\text{Alcohol}} + X_{\text{Acetate}}$) for (a) EtAc system and (b) IPAc system.

further separated in a decanter. In the aqueous phase, high purity water is removed. The stripper composition profiles indicate that high purity acetate can be achieved while recycling vapor back to the decanter with a composition close to the ternary azeotrope (Fig. 4). The distillation lines in the quaternary composition space (Fig. 4) show the tray composition of liquid and

Table 5
Comparisons of different designs

Case	(A)	(B)	(C)	(D)
Process configuration	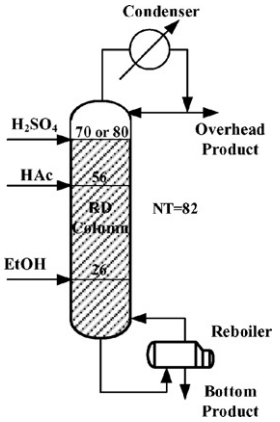	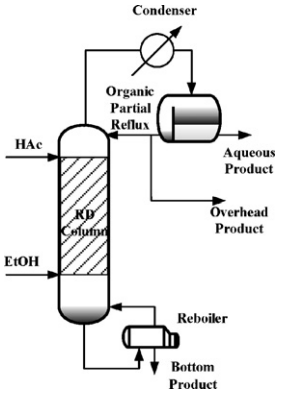	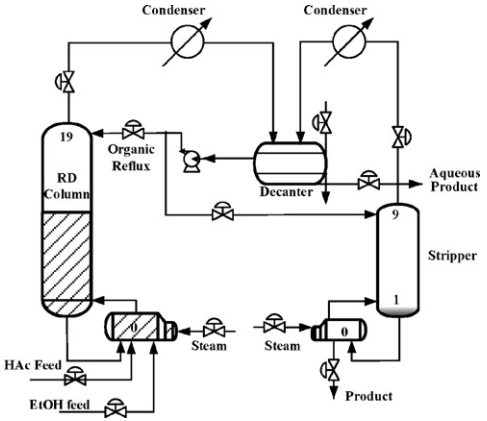	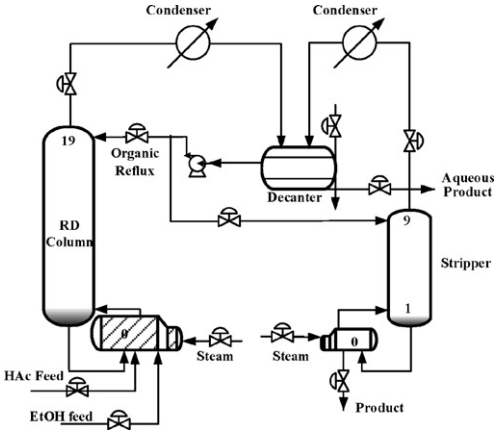
Authors	Kenig et al. (2001)	Klöker et al. (2004)	Proposed	Alternative to (C)
Remark	Experiment, homogeneous catalyst, 80 bubble cap trays	Experiment, single column with alternative internals and diameters	Simulation, two-column process heterogeneous catalyst	Simulation, catalyst in RD reboiler only
Achievement	HAc conversion: 68.5–86% X_{EtAc}–60 mol%	EtOH conversion: 36.2–91.7% $X_{EtAc} = 49.1$–93.1 wt%	HAc conversion: 100% $X_{EtAc} = 99$ mol%	HAc conversion: 94% $X_{EtAc} = 71.73$ mol%

Table 6
Comparison of steady-state designs for EtAc and IPAc systems with pure and azeotropic feed

System	(A) EtAc				(B) IPAc			
Feed	Pure		Impure		Pure		Impure	
No. of trays in rectifying section (N_r)	11		11		13		14	
No. of trays in reactive section (N_{rxn})	9		9		13		10	
No. of trays in stripping section (N_s)	9		9		7		7	
Column diameter (m)	RD	Stripper	RD	Stripper	RD	Stripper	RD	Stripper
	1.95	1.45	2.043	1.37	1.89	1.23	1.94	1.3
Reboiler duty in RD (kW)	4523.98		5113.4		3473.31		4014.17	
Reboiler duty in stripper (kW)	2195.68		1979.01		1370.90		1557.66	
Da	29.61		30.94		13.08		14.03	

vapor phase as well as the tie lines which indicates the composition in the organic and aqueous phases. Compared with other reactive distillation configurations, use of excessive alcohols to obtain a ternary water–alcohol–acetate mixture at the top of the RD column and the use of decanter to remove water are the keys in the development of these two esterification processes.

In order to validate the advantages of this current design over the other alternatives, two cases are also studied with simulations. One is to consider replacing the two columns with one single reactive distillation column, and the other is to put all the catalysts in the RD column to its reboiler which has expended volume than the original design to accommodate the extra catalysts originally in the RD column. The results are given in Table 5. From the results (Table 5(A) and (B) for experiments, (C) for simulation), it is obvious that the system with single RD column suffers from low conversion of HAc, low acetate concentration at the top, and off-spec effluents from the bottom. On the other hand (Table 5(D)), for system that has no catalyst in the RD column, the HAc in the bottom effluent is off from the specification and the resulting concentration of EtAc in the product is kind of low.

3.4. Comparison—pure feed vs. azeotropic feed

Although both feeds have water as impurity raging from 5% to 35%, it is interesting to find that the process characteristics are quite similar to that of the pure-feed designs. Table 6 summarizes numbers of trays, column diameters, reboiler duties, and Damkoler numbers for pure-feed design and azeotrpic feed designs for both EtAc and IPAc systems. For EtAc system, the configuration of the process flowsheet has only minor changes. Slight changes are found in the column diameters (the RD column and stripper) and in the heat duties of both systems. These changes result in a 5% increase of TAC for EtAc system and 8% increase in TAC for the IPAc system. The increase of TAC is mainly due to a small increase of the operational cost, e.g., energy cost to boilup excess water from the feeds. The increase of TAC is obviously insignificant. The detailed comparisons of the TACs are given in Fig. 5. From these results, we conclude that purifications of either the alcohols or the acetic acid is not necessary as far as the TAC is concerned.

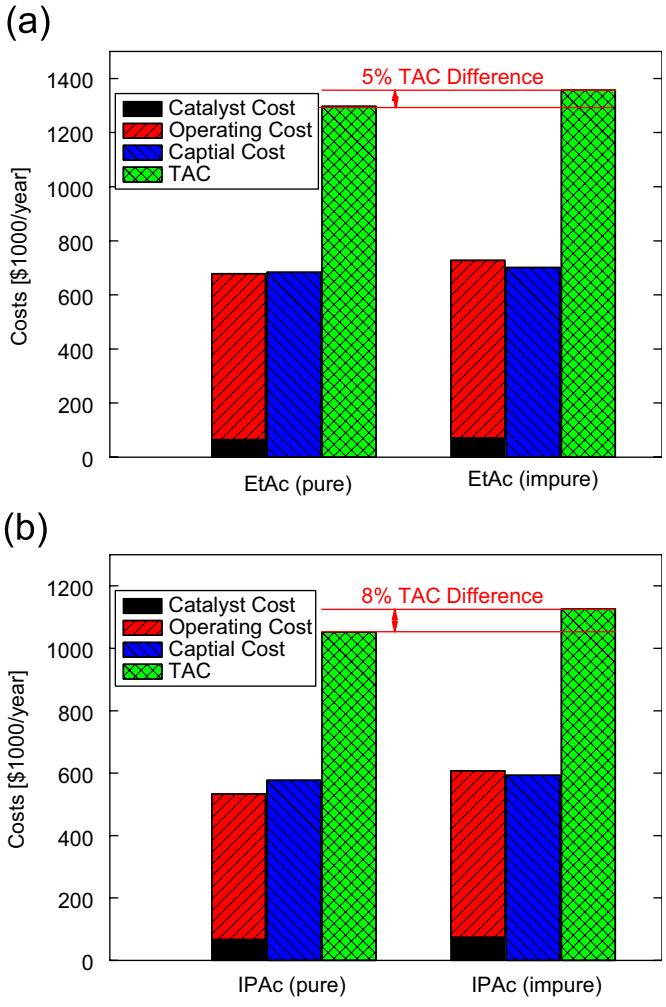

Fig. 5. Comparison of TACs for (a) EtAc System and (b) IPAc System.

4. Temperature control

In this section, a systematic approach is used to design the control structure for the EtAc and IPAc reactive distillation systems. Although studies on the simultaneous optimization of process design and control appeared in some late literature such as Sakizlis et al. (2004), Georgiadis et al. (2002), this study

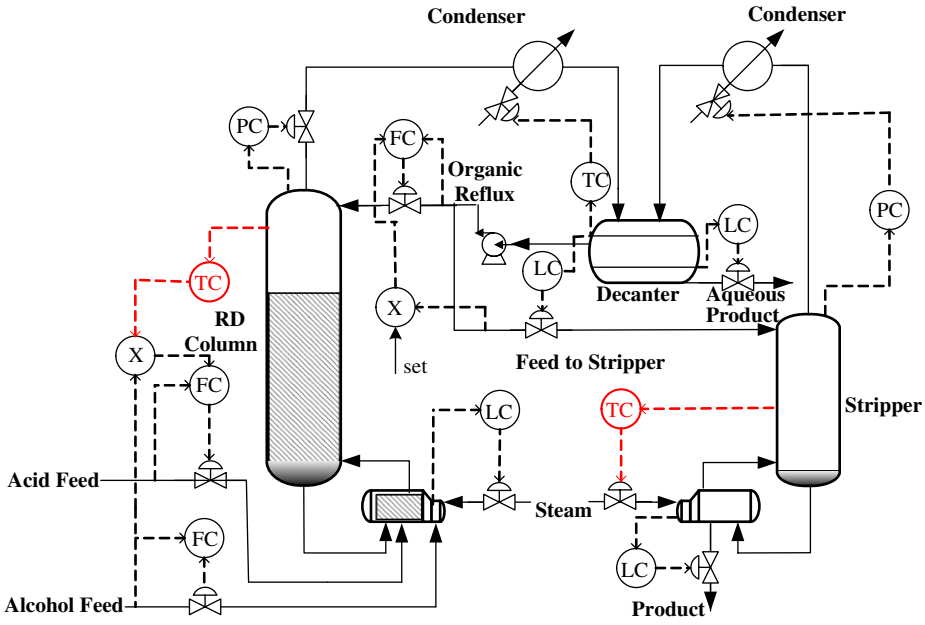

Fig. 6. Dual-temperature control configurations.

adopts the approach that control is designed after an economically optimal process being designed to ensure good operability under disturbances. The control objective is to maintain the acetate purity at 99 mol% while keeping the HAc impurity below 0.01 mol%. The fresh alcohol feed flow rate is the throughput manipulator. Production rate variations are handled using in this flow rate which is considered as a load disturbance in the subsequent study. In each of the system, there are 11 control degrees of freedom. They include: the reflux flow rate of the RD column, the distillate flow rate of the organic phase, the distillate flow rate of aqueous phase from the decanter, the product flow rate from the bottom of the stripper, two reboiler duties (i.e., RD column and stripper), the acid feed flow, the alcohol feed flow, two condenser duties, and vapor rate from the RD column. Among them, six degrees of freedoms are used for inventory control to keep the total materials in balance. They are: the RD column base level, the RD column pressure, decanter aqueous phase level, decanter organic phase level, stripper base level, and stripper pressure. For the remaining control degrees of freedom, one is used for the throughput manipulator and another for maintaining the decanter temperature. We are left with three degrees of freedom. Two of these, in theory, should be used for the control of two product compositions, water purity from the decanter and acetate composition at the bottoms of the stripper. The last degree of freedom is used to maintain stochiometric balance. Specific control structure is described in the next two sections.

4.1. Inventory related control

In these two processes, there are six inventory control loops. These six inventory control loops include the four level controls (i.e., bottom of RD column, organic phase in decanter, aqueous phase in decanter, bottom of stripping column) and two column pressures. These inventory loops are arranged as follows. The decanter level of the organic phase is controlled by manipulating the organic distillate flow rate (feed to the stripper), the level of the aqueous phase is controlled by the aqueous outlet flow, the stripper base level is controlled by the acetate product flow rate, and the RD column bottom level is controlled by manipulating the reboiler duty (because no outflow in the bottoms of the RD column). The stripper pressure is controlled by manipulating the condenser duty, and the RD column pressure is maintained by adjusting the overhead vapor rate (Fig. 6). Because the decanter is operated under subcooled condition, the decanter temperature is maintained at 40 °C by changing the condenser duty. The selection of the pairing for these inventory loops is based on the promptness of to the manipulation to the controlled variables.

4.2. Quality control and stoichiometric balance

As mentioned earlier, we are left with three control degrees of freedom for two product qualities as well as for maintaining stoichiometric balance. Because the water purity is determined by the tie line from the LL equilibrium and most of the tie lines point toward the water corner, the remaining manipulated variables have little impact on this product composition. Thus, instead of controlling the water purity, the reflux ratio is kept constant for the desired level of separation. Therefore, we have two control objectives: (1) controlling acetate product purity, and (2) maintaining stoichiometric balance. This leads to a 2×2 multivariable control system. Two remaining manipulated inputs are: (1) stripper heat duty, and (2) feed ratio ($F_{\mathrm{Acid}}/F_{\mathrm{Alcohol}}$). Dynamically, the two columns are separated by a decanter with a typically residence time of 20 min. These

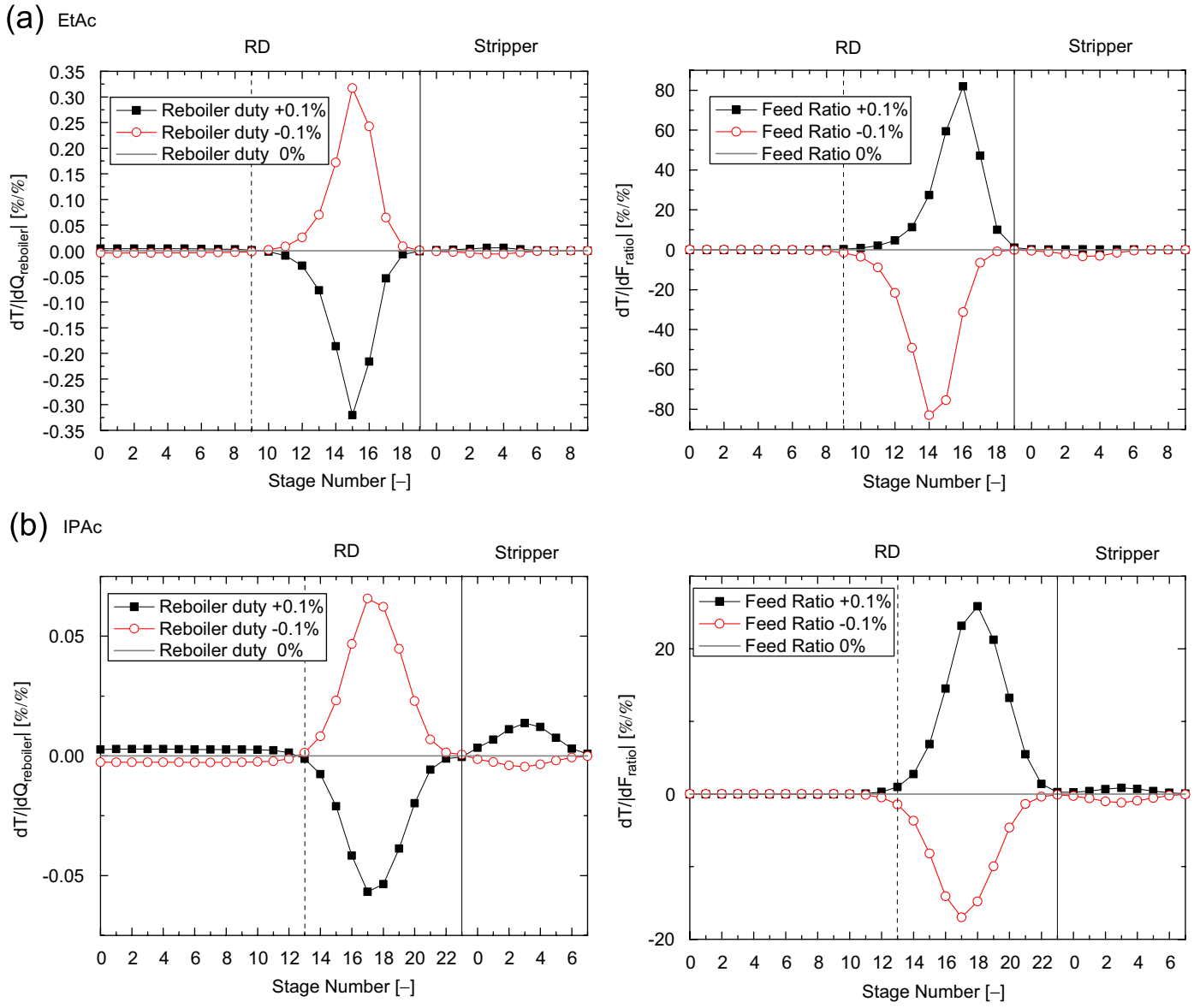

Fig. 7. Sensitivities of tray temperatures for ±0.05% manipulated variables changes (reactive zone indicated by two dotted lines).

two columns can be considered decoupled dynamically. Thus, decentralized control is employed for the product quality control and stoichiometric balance maintenance. This results in the following design procedures (Hung et al., 2006):

(1) Determine the manipulated variables and, in this case, they are the stripper heat duty and fresh feed ratio.
(2) Use the non-square relative gain (NRG) of Chang and Yu (1990) to select temperature control trays. The larger row sums of the NRG indicate potential temperature control tray.
(3) Use the relative gain array (RGA) for variable pairing.
(4) Performance sequential relay feedback test (Shen and Yu, 1994) to find the ultimate gain (K_u) and ultimate period (P_u).
(5) Use the Tyreus–Luyben tuning to set the tuning constant for the PI controllers. A simple version is $K_c = K_u/3$ and $\tau_I = 2P_u$.

4.3. Selection of temperature control trays

Sensitivity analyses are performed on theses two esterification reactive distillation systems (Fig. 7). In order to find the steady-state gains of tray temperature in the linear region, extremely small step changes (±0.05%) in the manipulated variables are made. Recall the two manipulated variables. One is the heat input to the stripper ($Q_{R,S}$) and the other is the fresh feed ratio (FR). For the EtAc system, an *increase* in $Q_{R,S}$ leads to a *decrease* in the tray temperatures of the reactive distillation column (Fig. 7). Note that in Fig. 7 the

Table 7
Process gain matrices, relative gain array, and tuning parameters for EtAc and IPAc systems under temperature control

	Controlled variables	Manipulated variables	Steady-state gain	RGA	Tuning parameter
EtAc	$T_{STR,3}$ $T_{RDC,15}$	F_{Acid}/F_{EtOH} $Q_{R,S}$	$\begin{bmatrix} T_{STR,3} \\ T_{RD,15} \end{bmatrix} = \begin{bmatrix} 0.242 & 3.34 \\ -12.844 & 222.686 \end{bmatrix} \begin{bmatrix} Q_{R,S} \\ FR \end{bmatrix}$	$Q_{R,S}$, F_{Acid}/F_{EtOH} $\Lambda = \begin{bmatrix} 0.5568 & 0.4432 \\ 0.4432 & 0.5568 \end{bmatrix} \begin{matrix} T_{STR,3} \\ T_{RD,15} \end{matrix}$	$Q_{R,S} - T_{STR,3}$: $K_c = 1.61$, $\tau_I = 3.05$ (min) $F_{Acid}/F_{EtOH} - T_{RDC,15}$: $K_c = 1.38$, $\tau_I = 180$ (min)
IPAc	$T_{STR,3}$ $T_{RDC,17}$	F_{Acid}/F_{IPOH} $Q_{R,S}$	$\begin{bmatrix} T_{STR,3} \\ T_{RD,17} \end{bmatrix} = \begin{bmatrix} 0.172 & 3.97 \\ -3.518 & 82.79 \end{bmatrix} \begin{bmatrix} Q_{R,S} \\ FR \end{bmatrix}$	$Q_{R,S}$, F_{Acid}/F_{IPOH} $\Lambda = \begin{bmatrix} 0.5048 & 0.4952 \\ 0.4952 & 0.5048 \end{bmatrix} \begin{matrix} T_{STR,3} \\ T_{RD,17} \end{matrix}$	$Q_{R,S} - T_{STR,3}$: $K_c = 19.17$, $\tau_I = 5.52$ (min) $F_{Acid}/F_{IPOH} - T_{RDC,18}$: $K_c = 2.9$, $\tau_I = 162.6$ (min)

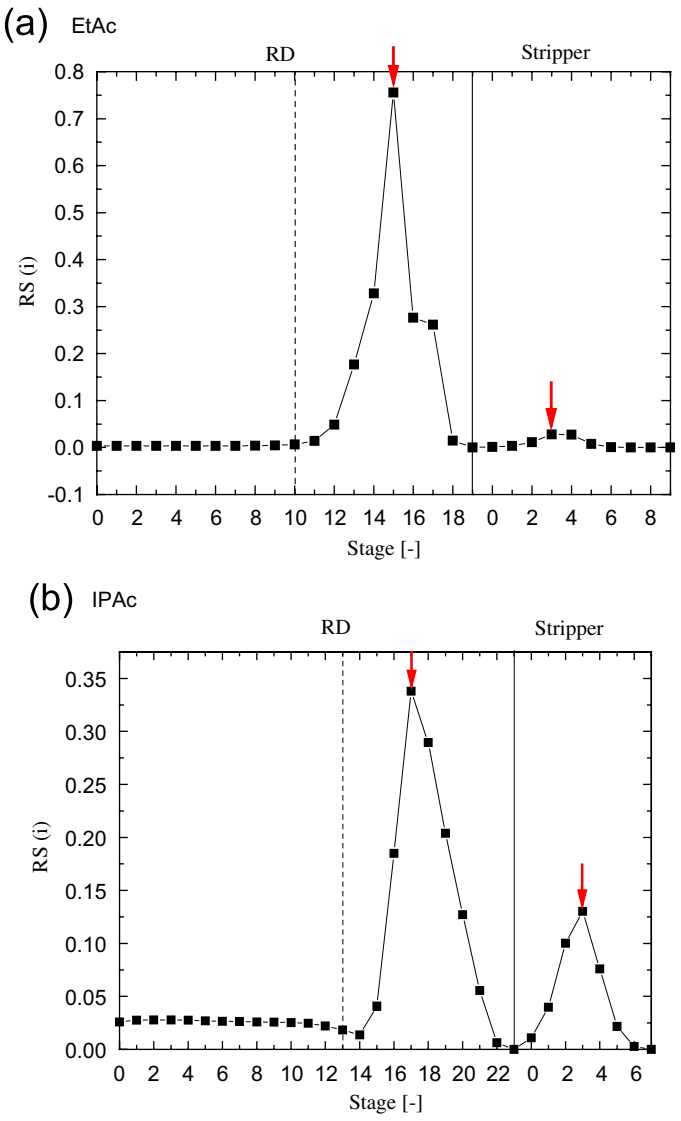

Fig. 8. Row sums of NRG for RD column and the stripper (selected temperature control trays indicates in arrows).

temperatures in the RD column and the stripper are combined and are labeled in the x-axis. This is a rather unusual phenomena which is a direct consequence of the process configuration. An increase in $Q_{R,S}$ results in a larger vapor rate from the stripper and subsequently condensed back to the decanter and this implies a larger recycle flow rate for the RD column. As for the acid feed ($F_{Acid}/F_{Alcohol}$) changes, an increase in the heavy reactant results in tray temperatures rise throughout the RD column while the stripper temperatures show little variation. The arguments also apply to the IPAc system as shown in Fig. 7.

The NRG is used to find the temperature control trays in each column. The largest row sum of the NRG in each column is selected as the temperature control trays. Fig. 8 shows the row sums for two systems thus, the controlled variables are:

EtAc: $T_{RDC,15}$ and $T_{STR,3}$,
IPAc: $T_{RDC,17}$ and $T_{STR,3}$.

4.4. Control structure and controller design

The next step is to find the variable pairing for the controlled and manipulated variables. Table 7 (4th column) gives the steady-state gain matrices from the linear analysis. The RGA (Bristol, 1966) is used for variable pairings. For the type II flowsheets (EtAc and IPAc), a stripper temperature is maintained using the heat input to the stripper and a temperature in the RD column is controlled using the ratio of fresh feeds into the RD column. (i.e., $T_{STR,3}$–$Q_{R,S}$ and $T_{RDC,15}$–F_{Acid}/F_{EtOH} for EtAc and $T_{STR,3}$–$Q_{R,S}$ and $T_{RDC,17}$–F_{Acid}/F_{IPOH} for IPAc). The relay feedback test (Shen and Yu, 1994) is used to find the ultimate gain (K_u) and the ultimate period (P_u) followed by the Tyreus–Luyben PI tuning rule. The identification-tuning step is carried out sequentially to find the controller settings for the PI controller. We find the sequential relay feedback autotuning procedure is very effective for these two reactive distillation processes. Table 7 summarizes the settings for these two reactive systems with two PI loops. It can be seen that the large reset time is associated with the feed ratio (FR) loop and the reset time for the heat input loop is relatively small. This implies we have two dynamically different speeds of responses, that is, the stoichiometric balance is maintained in a smooth manner while tight control is applied to the product purity.

4.5. Performance

Three disturbances, production rate changes and two feed composition variations (acetic acid and alcohol), are used to evaluate the control performance of these two esterification

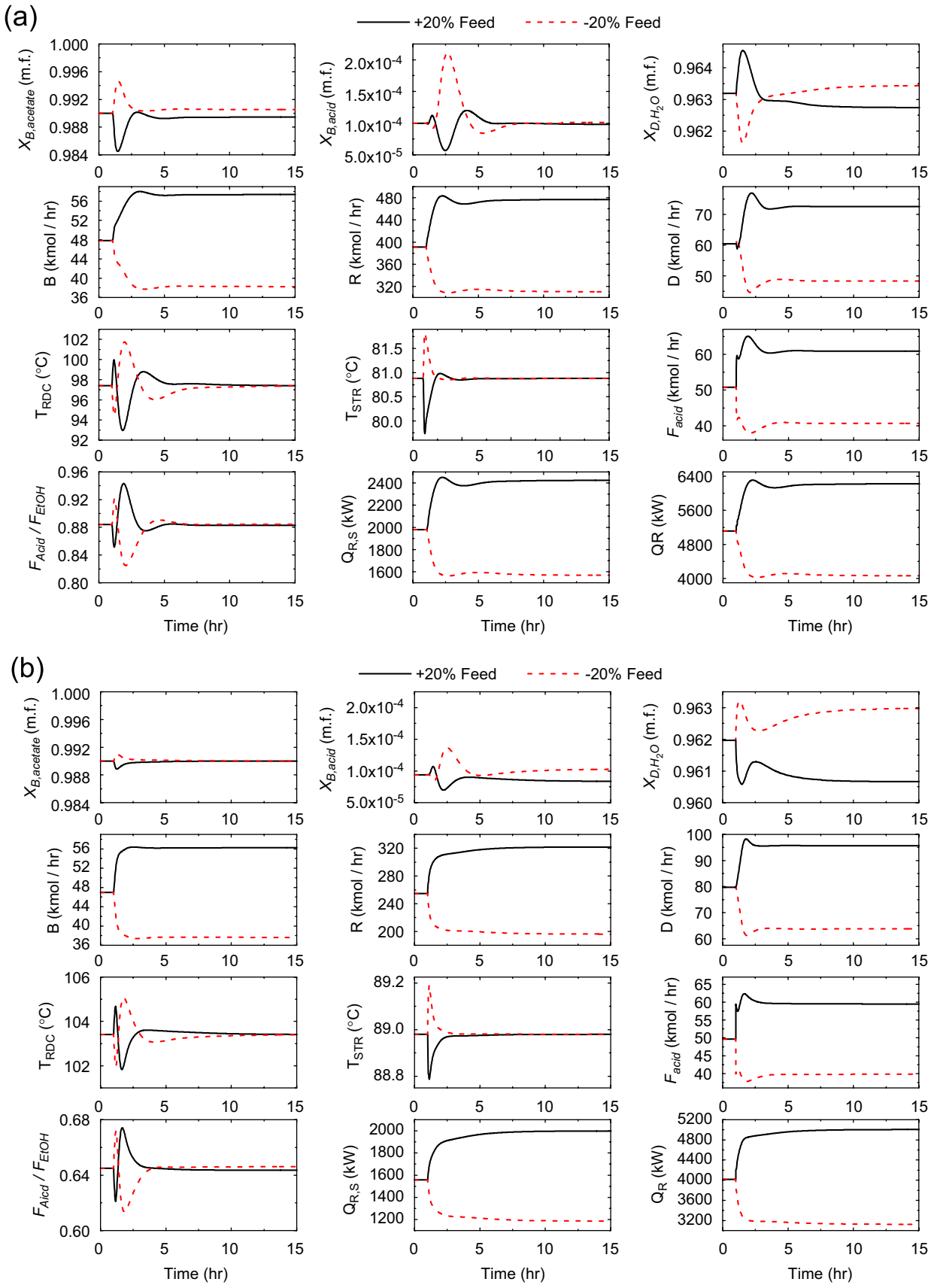

Fig. 9. Temperature control responses for ±20% production rate changes for (a) EtAc system and (b) IPAc system.

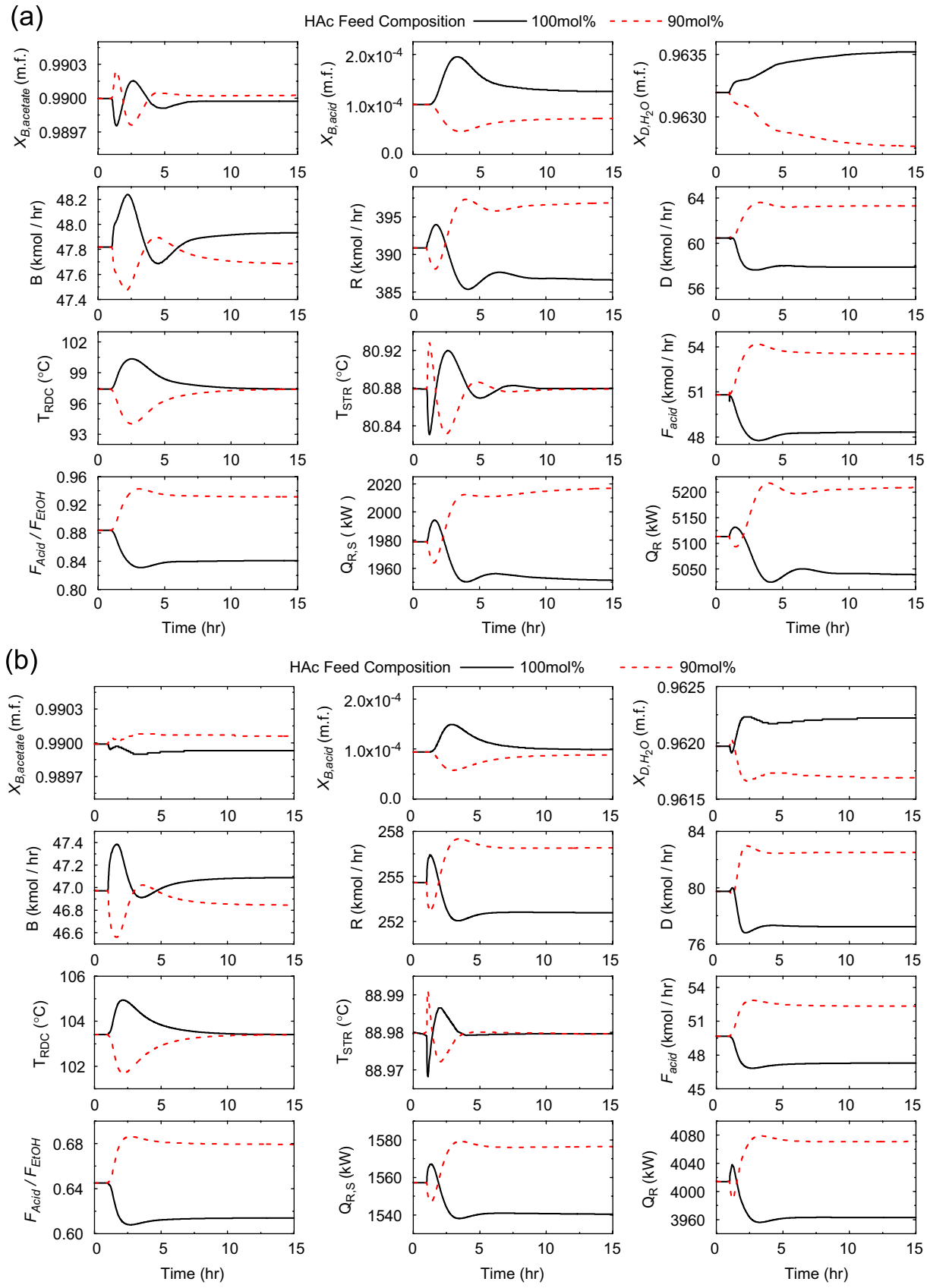

Fig. 10. Temperature control responses for ±5 mol% HAc feed composition changes for (a) EtAc system and (b) IPAc system.

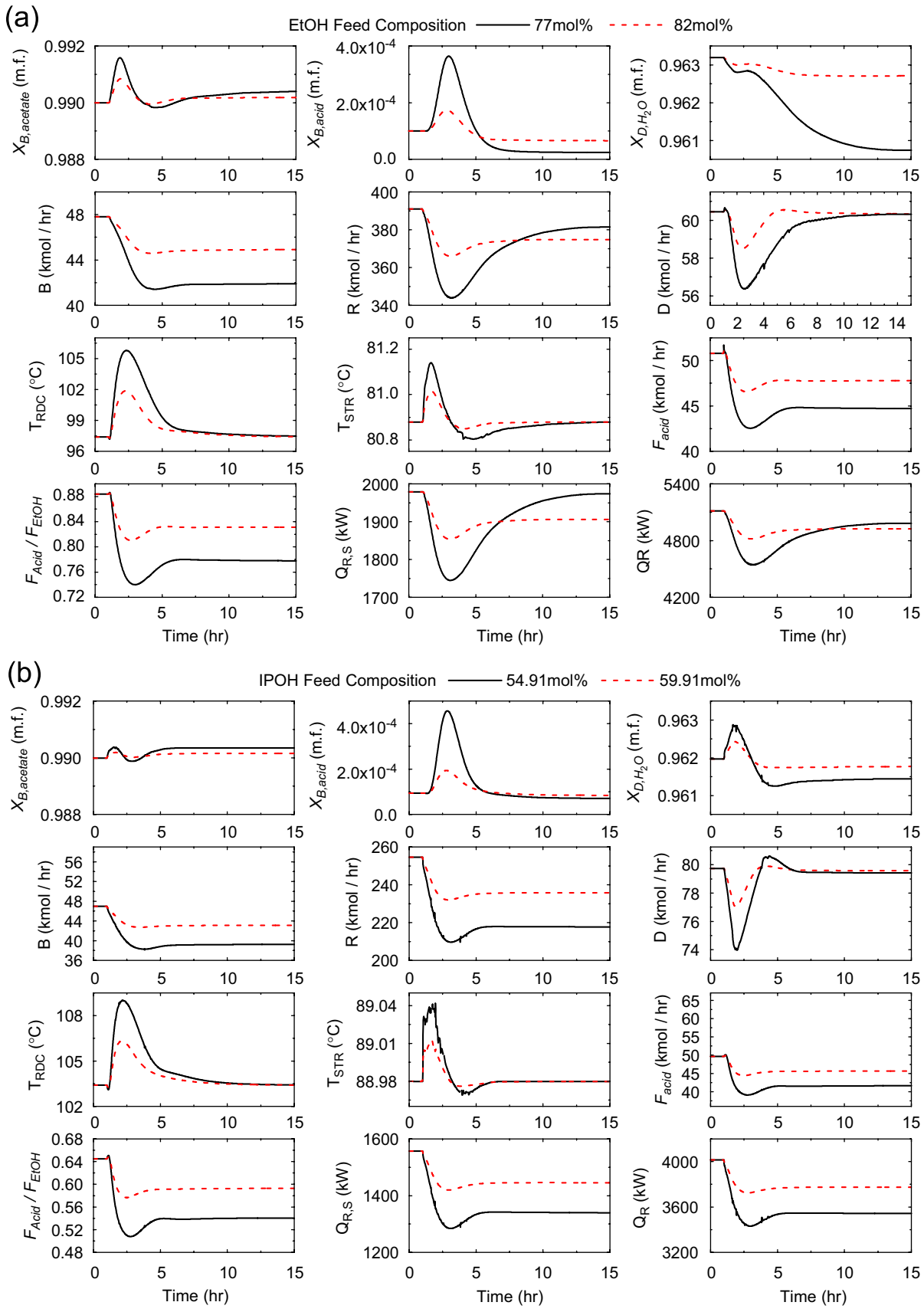

Fig. 11. Temperature control responses for −5 and −10 mol% alcohol feed composition changes for (a) EtAc system and (b) IPAc system.

Table 8
Process gain matrices, relative gain array, and tuning parameters for EtAc and IPAc systems under one-temperature-one-composition control

	Controlled variables	Manipulated variables	Steady-state gain	RGA	Tuning parameter
EtAc	$X_{B,\mathrm{EtAc}}$ $T_{\mathrm{RDC},15}$	$F_{\mathrm{Acid}}/F_{\mathrm{EtOH}}$ $Q_{R,S}$	$\begin{bmatrix} X_{B,\mathrm{EtAc}} \\ T_{\mathrm{RDC},15} \end{bmatrix} = \begin{bmatrix} 0.068 & 0.572 \\ -4.26 & 102.57 \end{bmatrix} \begin{bmatrix} Q_{R,S} \\ F_{\mathrm{Acid}}/F_{\mathrm{EtOH}} \end{bmatrix}$	$Q_{R,S}$, $F_{\mathrm{Acid}}/F_{\mathrm{EtOH}}$ $\Lambda = \begin{bmatrix} 0.742 & 0.258 \\ 0.258 & 0.742 \end{bmatrix}$ $\begin{matrix} X_{B,\mathrm{EtAc}} \\ T_{\mathrm{RDC},15} \end{matrix}$	$Q_{R,S} - X_{B,\mathrm{EtAc}}$: $K_c = 3.41$, $\tau_I = 11.51$ (min) $F_{\mathrm{Acid}}/F_{\mathrm{EtOH}} - T_{\mathrm{RDC},15}$: $K_c = 0.8$, $\tau_I = 303$ (min)
IPAc	$X_{B,\mathrm{IPAc}}$ $T_{\mathrm{RDC},18}$	$F_{\mathrm{Acid}}/F_{\mathrm{IPOH}}$ $Q_{R,S}$	$\begin{bmatrix} X_{B,\mathrm{IPAc}} \\ T_{\mathrm{RDC},18} \end{bmatrix} = \begin{bmatrix} 0.1514 & 0.7013 \\ -2.336 & 70.439 \end{bmatrix} \begin{bmatrix} Q_{R,S} \\ F_{\mathrm{Acid}}/F_{\mathrm{IPOH}} \end{bmatrix}$	$Q_{R,S}$, $F_{\mathrm{Acid}}/F_{\mathrm{IPOH}}$ $\Lambda = \begin{bmatrix} 0.866 & 0.133 \\ 0.133 & 0.866 \end{bmatrix}$ $\begin{matrix} X_{B,\mathrm{IPAc}} \\ T_{\mathrm{RDC},18} \end{matrix}$	$Q_{R,S} - X_{B,\mathrm{IPAc}}$: $K_c = 4.04$, $\tau_I = 6.63$ (min) $F_{\mathrm{Acid}}/F_{\mathrm{IPOH}} - T_{RDC,18}$: $K_c = 1.86$, $\tau_I = 447.6$ (min)

systems. The simple PI temperature control actually works quite well for these two systems as shown in Figs. 9–11. For ±20% production changes, the responses are rather symmetrical as shown in Fig. 9. The product composition settles in less than 10 h for both systems and steady-state offsets are quite small for the acetate products (∼ 0.1 mol% for EtAc and nil for IPAc). For ±5 mol% HAc feed composition changes, composition dynamics settle in ∼ 10 h and steady-state offsets in acetates are less than 0.01% as shown in Fig. 10. Moreover, symmetrical responses in the temperatures controlled tray temperatures (T_{RDC} and T_{STR}) and manipulated inputs (FR and $Q_{R,S}$) are observed. For −5 and −10 mol% alcohol feed composition disturbances, it takes around 10 h for the product composition to settle as shown in Fig. 11. The steady-state offsets in acetate is less than 0.04 mol% in all cases.

The results clearly indicate that the processes are resilient for moderate size rate as well as composition disturbances and decentralized PI control performs reasonably well for these dynamically decoupled systems

5. Composition control

If steady-state offset in acetate quality is not acceptable, composition control should be installed, instead. This leads to a one-temperature-one-composition control structure. Because the acetate product is withdrawn from the bottoms of the stripper, a composition controller is used while keeping the temperature controller for the RD column control. Similar to the dual-temperature control, the manipulated variables are feed ratio and stripper heat duty.

Once the control structure is determined, the RGA is computed for variable pairings (Table 8). The diagonal elements of the RGA is closer to unity as compared to dual-temperature control (Table 7) for both cases. Again, sequential relay feedback tests and autotuning are performed to find the PI controller settings as shown in Table 8. Similar to the settings for temperature control (Table 7), the reset times of feed ratio control loop are much larger than those of the heat duty control loop. Again, the control systems are designed in a systematic manner with a minimal complexity in the design steps, identification, tuning, and controller types.

The performance of the one-temperature-one-composition control is simulated by using Aspen Dynamics. For the composition measurement, 4 min of analyzer dead time is assumed. In general, the dynamics behaviors of these two systems under composition control (Figs. 12–14) are quite similar to that of the temperature control, except that zero steady-state offsets in the acetate composition. The speed of response of composition control for feed disturbance is almost the same as compared to that of temperature control. For the feed composition disturbances, the speed of responses for these two systems is little slower than that of the feed flow disturbances. The EtAc and IPAc systems take about 10–15 h to return to steady state with no error in the product composition (Figs. 13 and 14). It is found that, for composition disturbances, the feed ratio is adjusted automatically to accommodate the variation via the temperature controller in the RD column. Certainly, the steady-state offset in the acetate composition can be eliminated when a composition loop is used.

6. Conclusion

This paper proposes conceptual designs for two reactive distillation processes with azeotropic feed. The reactive distillations studied are for the production of ethyl acetate (EtAc) and isopropyl acetate (IPAc). A systematic design procedure is presented to improve the quantitative design based on the total annual cost (TAC). The ternary minimum boiling azeotrope and ranking of the boiling points leads to a reactive distillation column with a reactive zone and a rectifying section followed by a stripper, a type II reactive distillation configuration. For alcohol feeds below azeotrope composition (87 mol% for EtOH and 65 mol% for IPOH), the TACs only increase by a factor of 5% for EtAc system and 8% for IPAc system. This offers attractive alternatives for EtAc and IPAc productions.

Next, the issue of control strategies for reactive distillation is studied. Two control structures, dual-temperature control and one-temperature-one-composition control, are considered. The NRG is used to determine sensor locations and the RGA is used to characterize the interaction and, subsequently, determine corresponding controller structure. The autotune variation test is employed to determine ultimate gain (K_u) and ultimate period (P_u), and the Tyreus–Luyben tuning is used to find controller parameters. Since steady-state offsets in product composition may result in temperature control, the composition control is also devised. Good disturbance rejection is

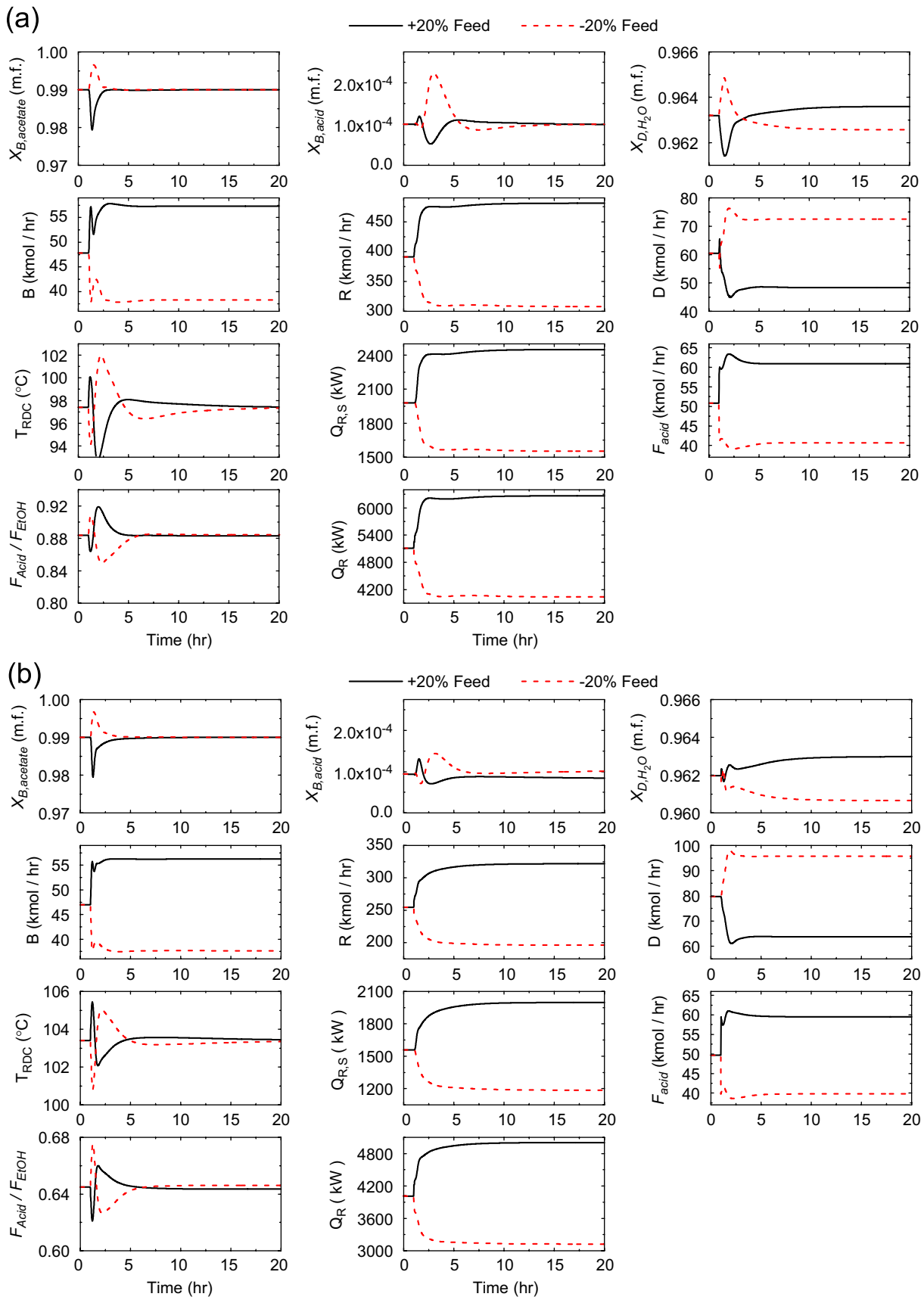

Fig. 12. Composition control responses for ±20% production rate changes for (a) EtAc system and (b) IPAc system.

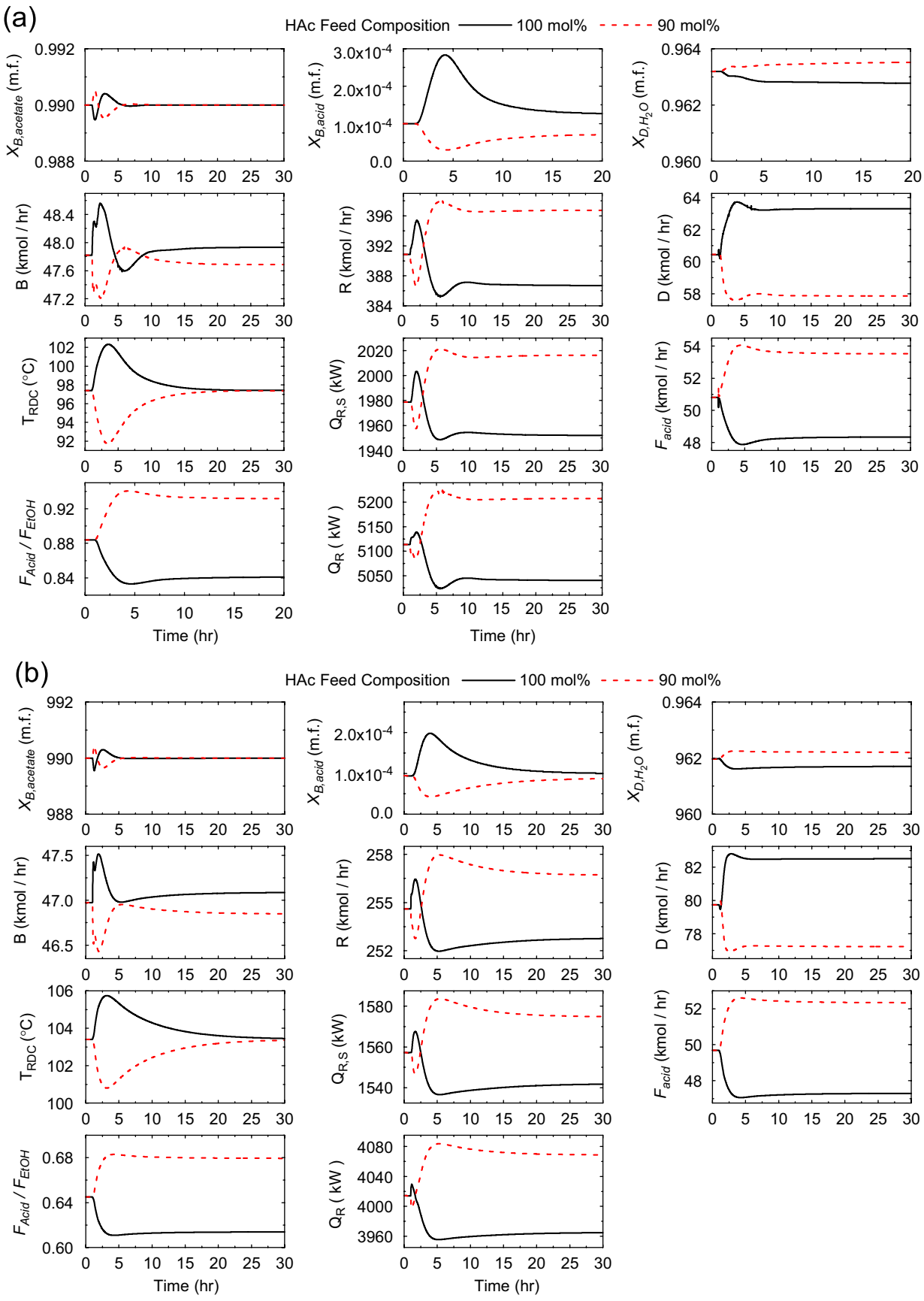

Fig. 13. Composition control responses for ±5 mol% HAc feed composition changes for (a) EtAc system and (b) IPAc system.

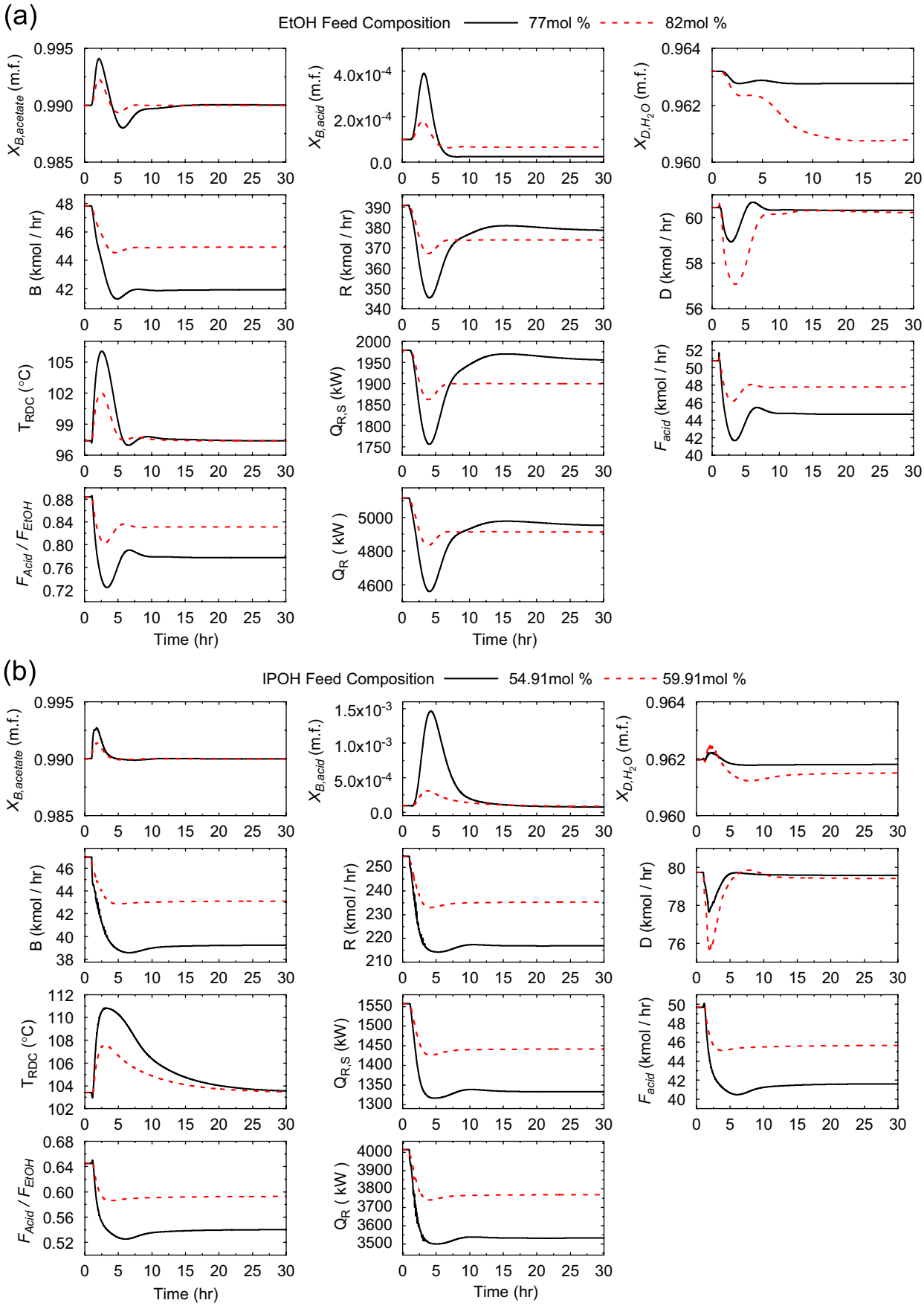

Fig. 14. Composition control responses for −5 and −10 mol% alcohol feed composition changes for (a) EtAc system and (b) IPAc system.

observed for these control schemes. From the simulation results of control, it comes to a conclusion that the processes are resilient for moderate-size rate as well composition disturbances and decentralized PI control perform reasonably well for these dynamically decoupled systems.

Notation

B	bottom flow rate (Type II: stripper)
D	distillate flow rate (Type II: aqueous phase flow rate)
EtAc	ethyl acetate
EtOH	ethanol
F_{Acid}	acid feed flow rate
F_{Alcohol}	alcohol feed flow rate
FR	feed ratio
HAc	acetic acid
IPAc	isopropyl acetate
IPOH	isopropanol
K_c	controller gain
K_p	process gain
K_u	ultimate gain
LL	liquid–liquid
m.f.	mole fraction
NF_{Acid}	acid feed location
NF_{Alcohol}	alcohol feed location
N_r	number of trays in the rectifying section
N_{rxn}	number of trays in the reactive section
NRG	non-square relative gain
N_s	number of trays in the stripping section
ORG	organic phase
P_u	ultimate period
$Q_{R,S}$	reboiler duty of the stripper
RD	reactive distillation
RDC	reactive distillation column
RR	reflux ratio
STR	stripper
$T_{\text{RDC},i}$	ith tray temperature in reactive distillation column
$T_{\text{STR},i}$	ith tray temperature in stripper
TAC	total annual cost
X	mole fraction

Acknowledgment

This work is supported by Ministry of Economic Affair under Grant 93-EC-17-A-09-S1-019.

References

Alejski, K., Duprat, F., 1996. Dynamic simulation of the multicomponent reactive distillation. Chemical Engineering Science 51, 4237–4252.

Aspen Dynamics and Aspen Plus, 2001. Release 11.1, Aspen Technology, Inc., Cambridge, MA, USA.

Bock, H., Jimoh, M., Wozny, G., 1997. Analysis of reactive distillation using the esterification of acetic acid as an example. Chemical Engineering & Technology 20, 182–191.

Bristol, E.H., 1966. On a new measure of interaction for multivariable process control. IEEE Transactions on Automatic Control AC11 (1), 133.

Chang, J.W., Yu, C.C., 1990. The relative gain for non-square multivariable system. Chemical Engineering Science 45, 1309–1323.

Chang, Y.A., Seader, J.D., 1988. Simulation of continuous reactive distillation by a homotopy-continuation method. Computers & Chemical Engineering 12, 1243–1255.

Gadewar, S.B., Malone, M.F., Doherty, M.F., 2002. Feasible region for a countercurrent cascade of vapor. A.I.Ch.E. Journal 48, 800–814.

Georgiadis, M.C., Schenk, M., Pistikopoulos, E.N., Gani, R., 2002. The interations of design, control and operability in reactive distillation systems. Computers & Chemical Engineering 26, 735–746.

Giessler, S., Savilov, R.Y., Pisarenko, R.Y., Serafimov, L.A., Hasebe, S., Hashimoto, I., 2001. Systematic structure generation for reactive distillation processes. Computers & Chemical Engineering 25, 49–60.

Hangx, G., Kwant, G., Maessen, H., Markusse P., Urseanu I., 2001. Reaction kinetics of the esterification of ethanol and acetic acid towards ethyl acetate. Deliverable 22, Intelligent Column Internals for Reactive Separations (INTINT). Technical Report to the European Commission.

Hayden, J.G., O'Connell, J.P., 1975. A generalized method for predicting second viral coefficients. Industrial & Engineering Chemistry Process Design and Development 14, 209–216.

Hooke, R., Jeeves, T.A., 1966. Direct search of numerical and statistical problems. Journal of the ACM 8, 212–229.

Horsley, L.H., 1973. Azeotropic Data—III, Advances in Chemistry Series No. 116, American Chemical Society, Washington, DC, USA.

Hung, S.B., Lee, M.J., Tang, Y.T., Chen, Y.W., Lai, I.K., Hung, W.J., Huang, H.P., Yu, C.C., 2006. Control of different reactive distillation configurations. A.I.Ch.E. Journal 52, 1423–1440.

Kenig, E.Y., Bäder, H., Górak, A., Beßling, B., Adrian, T., Schoenmakers, H., 2001. Investigation of ethyl acetate reactive distillation process. Chemical Engineering Science 56, 6185–6193.

Keyes, D.B., 1932. Esterification processes and equipment. Industrial and Engineering Chemistry 24, 1096–1103.

Klöker, M., Kenig, E.Y., Górak, A., Markusse, A.P., Kwant, G., Moritz, P., 2004. Investigation of different column configurations for the ethyl acetate synthesis via reactive distillation. Chemical Engineering and Processing 43, 791–801.

Sakizlis, V., Perkins, J.D., Pistikopoulos, E.N., 2004. Recent advances in optimization-based simultaneous process and control design. Computers & Chemical Engineering 28, 2069–2086.

Shen, S.H., Yu, C.C., 1994. Use of relay-feedback test for automatic tuning of multivariable systems. A.I.Ch.E. Journal 40, 627–646.

Simandl, J., Svrcek, W.Y., 1991. Extension of the simultaneous-solution and inside–outside algorithms to distillation with chemical reactions. Computers & Chemical Engineering 15, 337–348.

Tang, Y.T., Huang, H.P., Chien, I.L., 2003. Design of a complete ethyl acetate reactive distillation system. Journal of Chemical Engineering of Japan 36, 1352.

Tang, Y.T., Chen, Y.W., Huang, H.P., Yu, C.C., Huang, S.B., Lee, M.J., 2005. Design of reactive distillations for acetic acid esterification with different alcohols. A.I.Ch.E. Journal 51, 1683–1699.

Vora, N., Daoutidis, P., 2001. Dynamics and control of an ethyl acetate reactive distillation column. Industrial & Engineering Chemistry Research 40, 833–849.